

Electronic structure, phase stability and chemical bonding in Th_2Al and Th_2AlH_4

P. Vajeeston^{1*}, R. Vidya¹, P. Ravindran¹, H. Fjellvåg^{1,2}, A. Kjekshus¹ and A. Skjeltorp²

¹*Department of Chemistry, University of Oslo, Box 1033, Blindern, N-0315, Oslo, Norway.*

²*Institute of Energy Technology, P.O.Box 40, Kjeller, N-2007, Norway.*

(November 6, 2018)

Abstract

We present the results of theoretical investigation on the electronic structure, bonding nature and ground state properties of Th_2Al and Th_2AlH_4 using generalized-gradient-corrected first-principles full-potential density-functional calculations. Th_2AlH_4 has been reported to violate the "2 Å rule" of H-H separation in hydrides. From our total energy as well as force-minimization calculations, we found a shortest H-H separation of 1.95 Å in accordance with recent high resolution powder neutron diffraction experiments. When the Th_2Al matrix is hydrogenated, the volume expansion is highly anisotropic, which is quite opposite to other hydrides having the same crystal structure. The bonding nature of these materials are analyzed from the density of states, crystal-orbital Hamiltonian population and valence-charge-density analyses. Our calculation predicts different nature of bonding for the H atoms along a and c . The strongest bonding in Th_2AlH_4 is between Th and H along c which form dumb-bell shaped H-Th-H subunits. Due to this strong covalent interaction there is very small amount of electrons present between H atoms along c which makes repulsive interaction between the H atoms smaller and this is the precise reason why the 2 Å rule is violated. The large difference in the interatomic distances between the interstitial region where one can accommodate H in the ac and ab planes along with the strong covalent interaction between Th and H are the main reasons for highly anisotropic volume expansion on hydrogenation of Th_2Al .

PACS numbers: 71., 81.05.Je, 71.15.Nc, 71.20.-b

I. INTRODUCTION

Hydrides of intermetallics have been extensively studied because of their applications in re-chargeable batteries. Unfortunately, most metals that absorb large amounts of hydrogen are either heavy or expensive.¹ Consequently, there is a constant search for hydrides that may be suitable for practical applications. First of all, it is very important to understand how crystal structural evolution takes place in the course of hydrogenation. Numerous studies have been done to explain observed stabilities, stoichiometries, and preferred H sites in hydrides of metallic and intermetallic compounds. Structural studies of hydrides have provided empirical rules² that can be used to predict the stability of the H sublattice in a given metal configuration. A survey of stable hydrides show that the H–H distance does not go below 2.1 Å (the 2 Å rule) with a minimum radius of 0.4 Å for the inter-site to be used for the accommodation of H. These rules have been used to predict new hydrides whose existence is verified experimentally.^{1–3}

The review of Yvon and Fischer⁴ states that Th_2AlH_4 ⁵ and K_2ReH_9 ^{4,6} violate the 2 Å rule, the shortest H–H separation being 1.79, and 1.87, respectively. K_2ReH_9 is classified among complex transition metal hydrides, which comprise highly covalent solids with nonmetallic properties. Th_2AlH_4 , on the other hand, has metallic character.

Th_2Al ⁷ together with Zr_2Fe , Zr_2Co and Zr_2Ni crystallize in the CuAl_2 -type structure, whereas their hydrides form rather different crystal structures. Zr_2Fe and Zr_2Co form the isostructural deuterides Zr_2MD_5 ($\text{M} = \text{Fe}, \text{Co}$)⁸ with a change in symmetry from $I4/mcm$ to $P4/ncc$ on deuteration. Th_2AlH_4 ^{5,9} and $\text{Zr}_2\text{NiH}_{4.74}$ ¹⁰ are formed without any change in the symmetry from their parent structures. Th_2AlH_4 belongs to the exclusive class which does not obey the 2 Å rule. The lattice expansion along a and c has proved to be highly anisotropic on hydrogenation of Th_2Al . In order to shed light on this effect we need theoretical understanding about bonding nature in this compound. Further, the understanding of the lattice expansion and distortion during hydrogenation will be important for the evaluation of stability of the hydride. So, we have made detailed study of Th_2Al and Th_2AlH_4 by first-principle calculations.

Two different powder neutron diffraction (PND) of Th_2AlH_4 give different H-H separations, *viz.* the older⁵ value is 1.79 Å and the more recent⁹ value is 1.97 Å. So one aim of this study has been to solve this discrepancy. In principle, the stability of hydrides can be evaluated directly from a theoretical study of the total energy. However, owing to the complexity of the structure of transition metal hydrides, no reliable theoretical heat of formation has hitherto been reported.¹¹ Nakamura *et al.*¹¹ were the first to calculate heat of formation. However, these authors obtained positive and unrealistically large heat of formation even for stable La-Ni based hydrides except for $(\text{La}_2\text{Ni}_{10}\text{H}_{14})$.^{12–14} This unfavorable result clearly indicates that local relaxation of the metal atoms surrounding the hydrogens must be included in the calculations in order to predict the structural stability parameters. Hence our calculations take into account local relaxation by optimizing the atom positions globally.

We present the electronic structure of Th_2Al and Th_2AlH_4 , obtained by the full-potential linearized-augmented plane wave (FPLAPW) method. A central feature of the paper is the evaluation of the electronic structure and bonding characteristics on introduction of H into the Th_2Al matrix. In addition to regular band-structure data, we also provide crystal

orbital Hamiltonian population (COHP)^{15,16} results to illustrate the chemical bonding in more detail.

This paper is organized as follows. Details about the involved structure and computational method are described in Sec. II. Sec. III gives the results of the calculations and comparisons with the experimental findings. Conclusions are briefly summarized in Sec. IV.

II. STRUCTURAL DETAILS

Th₂Al and Th₂AlH₄ crystallize in space group *I4/mcm* with the lattice parameters $a = 7.618$, $c = 5.862 \text{ \AA}$ ¹⁷ for Th₂Al and $a = 7.626$, $c = 6.515 \text{ \AA}$ for Th₂AlH₄⁹ The crystal structure of Th₂AlH₄ is illustrated in Fig. 1. The crystal structure of Th₂Al contains four crystallographically different interstitial sites, which are the suitable sites for hydrogen accommodation, *16l* and *4b* each coordinated to four Th, *32m* coordinate to three Th and one Al *16k* coordinate to two Th and two Al. Each *16l* based intersite tetrahedra share a common face with another *16l*-based tetrahedron, whereas the *4b*-based tetrahedron shares each of its four faces with *16l*-based tetrahedra. Some of the tetrahedral intersites are closely separated owing to the face sharing of the coordination polyhedra. According to the experimental findings,^{5,9} the *16l* sites are fully occupied in Th₂AlD₄, and also the structure is completely ordered.

A. Computational details

In our calculations we use the full-potential linearized augmented plane wave (FP-LAPW) method in a scalar relativistic version without spin-orbit coupling as embodied in the WIEN97 code.¹⁸ In brief, this is an implementation of density-functional theory (DFT) with different possible approximations for the exchange and correlation potential, including the generalized-gradient approximation (GGA). The Kohn-Sham equations are solved using a basis of linearized augmented plane waves.¹⁹ For the exchange and correlation potential, we used the Perdew and Wang²⁰ implementation of GGA. For the potential and charge density representations, inside the muffin-tin spheres the wave function are expanded in spherical harmonics with $l_{max} = 10$, and non spherical components of the density and potential are included up to $l_{max} = 6$. In the interstitial region they are represented by Fourier series and thus they are completely general so that such a scheme is termed full-potential calculation. The present calculations we used muffin-tin radii of 2.5, 2.1 and 0.9 Bohr for Th, Al and H respectively.

The basis set includes *7s*, *7p*, *6d* and *5f* valence and *6s* and *6p* semi-core states for Th, *3s*, *3p* valence and *2p* semi-core states for Al and *1s* states for H. These basis functions were supplemented with local orbitals²¹ for additional flexibility to the representation of the semi-core states and for generalization of the linearization errors. We have included the local orbitals for Th *6s*, *6p* and Al *2p* semicore states. In all our calculations we have used tetrahedron method on a grid of 102 **k** points in the irreducible part of the hexagonal Brillouin zone (IBZ),²² which corresponds to 1000 **k** points in the whole Brillouin zone. The calculations are done at several cell volumes (around the equilibrium volume) for both Th₂Al and Th₂AlH₄ and corresponding total energies are evaluated self-consistently by iteration to an

accuracy of 10^{-6} Ry./cell. Similar densities of \mathbf{k} points were used for the force minimization and c/a optimization calculations.

In order to measure the bond strengths we have computed the COHP¹⁶ which is adopted in the TBLMTO-47 package.^{23,24} COHP is the density of states weighted by the corresponding Hamiltonian matrix elements, which if negative indicates a bonding character and positive indicates an anti-bonding character. The simplest way to investigate the bonding between two interacting atoms in the solid would be to look at the complete COHP between them, taking all valence orbitals into account. However, it may sometimes be useful to focus on pair contributions of some specific orbitals.

III. RESULT AND DISCUSSION

The H–H separation is one of the most important factors in identifying the potential candidate for hydrogen storage, because if the H-H separation is small one can accommodate more H within a small region. From this point of view, Th_2AlH_4 may be considered as a potential candidate for storing H. To the best of our knowledge no theoretical or experimental attempts have been made to study cohesive properties like heat of formation (ΔH), cohesive energy (E_{coh}), bulk modulus (B_0) and its pressure derivative (B'_0) for this compound. Hence, this is the first theoretical attempt to study the ground state properties and bonding in this compound.

A. Structural optimization from total energy studies

In order to analyze the effect of hydrogenation on the crystal structure of Th_2Al and to verify the discrepancy between the experimentally observed H-H separation, we have optimized the structural parameters for Th_2Al and Th_2AlH_4 . For this purpose, first we have relaxed the atomic positions globally using the force-minimization technique, by keeping experimental c/a and cell volume (V_0) fixed to experimental values. Then the theoretical equilibrium volume is determined by fixing optimized atomic positions and experimental c/a , and varying the cell volume by $\pm 10\%$ of V_0 . Finally the optimized c/a ratio is obtained by a $\pm 2\%$ variation in c/a ratio (in steps of 0.005), while keeping the theoretical equilibrium volume fixed. It is important to note that experimentally observed lattice parameters are almost same, while the atomic position of H alone differs between the two experimental results (according to Bergsma *et al.*⁵ H coordinates are 0.368, 0.868, 0.137 and Sørby *et al.*⁹ give 0.3707, 0.8707, 0.1512). The total energy *vs.* cell volume and c/a ratio curves for Th_2Al and Th_2AlH_4 are shown in Figs. 2 and 3, respectively. From these illustrations it is clear that the equilibrium structural parameters obtained from our theoretical calculations are in very good agreement with those obtained recently by PND measurements.⁹

The optimized atomic positions along with the corresponding experimental values are given in Table I. Table II gives calculated lattice parameters and interatomic distances, along with corresponding experimental values for both Th_2Al and Th_2AlH_4 . The theoretically estimated equilibrium volume is underestimated by 0.27% for Th_2Al and 1.8 % for Th_2AlH_4 . The underestimation of bond length in the present study is partly due to the limitation of local density approximation used in the calculations and also neglect of the zero-point motion

and thermal expansions. The difference between the experimental values may be due to the poor resolution of the earlier(1961) PND data⁵.

B. Cohesive properties

The method of calculation for cohesive properties for intermetallic compounds are well described in Refs. 25–27 The cohesive energy is a measure of the force that binds atoms together in the solid state. The cohesive energy of a system is defined as the sum of the total energy of constituent atoms at infinite separation minus the total energy of the particular system. This is a fundamental property which has long been the subject of theoretical approaches. The chemical bonding in intermetallic compounds is a mixture of covalent, ionic and metallic bonding and therefore the cohesive energy can not be determined reliably from simple models. Thus, first principle calculations based on DFT have become a useful tool to determine the cohesive energy of solids. For the study of phase equilibrium the cohesive energy is more descriptive than the total energy, since the latter includes a large contribution from electronic states that do not play a role in bonding. From our cohesive energy calculations we get $E_{coh} = 0.15, 0.185$ eV/atom for Th_2Al and Th_2AlH_4 respectively, indicating that hydrogenation enhances the bond strength in Th_2Al .

The formation energy (ΔH) is introduced in order to facilitate a comparison of system stability. ΔH is defined as the total energy difference between the compound and weighted sum of the corresponding total energy of the constituents. For the ΔH calculations, we used the total energy value of 2.320 Ry for the hydrogen molecule which was calculated with the von Barth-Hedin exchange-correlation potential.²⁸ ΔH provides information about the stability of Th_2Al towards hydrogenation. The calculated ΔH values for La-Ni based hydrides,¹¹ were almost double the experimental^{12–14} ΔH . As the LMTO-ASA method was used in this study, this discrepancy is expected because the internal relaxation of the atoms was not taken into account and the interstitial potential is not well represented in LMTO-ASA method. Therefore, ΔH calculated by using the full-potential method should be more reliable. Our calculated values for E_{coh} and ΔH are given in Table III. Since (ΔH) is more negative and E_{coh} is higher for Th_2AlH_4 than for Th_2Al , we can conclude that Th_2AlH_4 is more stable than Th_2Al . However, no experimental ΔH values for Th_2Al and Th_2AlH_4 , are available, but we note that our calculated ΔH is close to the experimentally observed values of other Th-based hydrides, like ThNi_5H_4 , ThCo_5H_4 and ThFe_5H_4 all having the ΔH value of -36.63 kJ/(mol-H).²⁹

The bulk modulus of Th_2Al and Th_2AlH_4 was obtained by self-consistent total energy calculations for 8 different volumes within the range of V/V_0 from 0.75 to 1.10 (see Fig. 2). From the derivative of total energy with respect to the volume, the calculated bulk modulus for Th_2Al is 93.42 GPa and for Th_2AlH_4 is 111.36 GPa. The corresponding pressure derivative of the bulk modulus (B'_0) are 3.43 and 3.51, respectively. The enhancement in B_0 value in the hydrogenated phase indicates that hydrogen plays an important role in bonding behavior of Th_2AlH_4 . In particular, the hydrogenation enhances the bond strength, and hence the change in volume with hydrostatic pressure decreases with hydrogenation. This conclusion is consistent with the observation made from our calculated heat of formation and cohesive energy for Th_2Al and Th_2AlH_4 .

C. Anisotropic behavior

For compounds which maintains the basic structural frame work, the occupancy of hydrogen in interstitial sites is determined by its chemical environment (different chemical affinity for the elements in the coordination sphere also results in different occupancy). Although the H atom is small and becomes even smaller by chemical bonding to the host, it may deform and stress the host metal considerably depending upon the chemical environment. Lattice expansion usually of the order of 5 to 30%, often anisotropic, results from hydride formation. The maximum volume expansion observed for CeRu_2 to CeRu_2D_5 (37%) is due to a hydrogen induced electron transition as shown by XPS measurements.³⁰ A lattice contraction upon hydrogenation has so far only been observed for ThNi_2 to ThNi_2D_2 (2.2%). For most hydrides formed from intermetallic compounds the crystal structure usually changes with a loss of symmetry.³¹ In general the symmetry decreases as a function of hydrogen content and increases as a function of temperature. However, on hydrogenation of Th_2Al the symmetry remains unchanged.

The volume expansion during hydrogenation of Th_2Al is 12.47% ($\Delta V/\text{H atom}$ is 10.32\AA^3). This volume expansion is strongly anisotropic and proceeds predominantly perpendicular to the basal plane of the tetragonal unit cell; $\Delta a/a = 0.026\%$, $\Delta c/c = 12.41\%$. This indicates a relatively flexible atomic arrangement in the [001] direction. In spite of the isostructurality between Th_2Al , Zr_2Fe (hydrated: Zr_2FeH_5)⁸ and Zr_2Co (hydrated: $\text{Zr}_2\text{CoH}_{4.82}$)³² the latter two exhibit a quite opposite anisotropic behavior in that the the unit cell expands exclusively along the basal plane. The c/a ratio plays an important role for the structural properties of intermetallic compounds including metal hydrides. For example, in the case of Zr_2Fe ⁸, Zr_2Co ³², Zr_2Ni ^{10,33} and Th_2Al c/a is 0.878, 0.867, 0.812 and 0.7695 respectively, and for the corresponding hydrides Zr_2FeH_5 ,¹⁰ $\text{Zr}_2\text{CoH}_{4.82}$,¹⁰ $\text{Zr}_2\text{NiH}_{4.74}$ ¹⁰ and Th_2AlH_4 c/a is 0.810, 0.815, 0.833 and 0.8543 respectively (see Fig. 4). The increase in c/a for $\text{Zr}_2\text{CoH}_{4.82}$ and Zr_2FeH_5 compared with the corresponding unhydrated parents is smaller than that for other compounds. On hydrogenation, the increase in c/a ratio for Th_2Al is considerably larger than for Zr_2Ni , which may be the reason why the former retains the symmetry on hydrogenation. Our calculations describe well the anisotropic changes in the crystal structure on hydrogenation of Th_2Al (see Table II). The c/a ratio increases almost linearly (Fig. 4) on going from Zr_2Fe to Th_2Al whereas the corresponding hydrides show the opposite behavior. Hence, it appears that the systematic variation in c/a plays a major role in deciding the crystal structure for the CuAl_2 -type hydrides. When $c/a < 0.825$ the symmetry is changed from $I4/mcm$ to $P4/ncc$ on hydrogenation, whereas when $c/a > 0.825$ the crystal symmetry is apparently not affected.

D. Electronic structure

In order to understand the changes in the electronic bands on hydrogenation of Th_2Al we show the energy band structure for Th_2Al and Th_2AlH_4 in Fig. 5a and *b* respectively. The illustration clearly indicates that inclusion of H in the Th_2Al matrix has a noticeable impact on the band structure, mainly in the valence band. The two lowest lying broad bands in Fig. 5a originate from Al 3s electrons. As the unit cell contains two formula units, eight electrons are additionally introduced when Th_2AlH_4 is formed from Th_2Al . These

electrons form four additional bands (Fig. 5b), a large deformation of the band structure is introduced by the of hydrogen in the Th_2Al lattice. These bands become localized, the lowest lying energy band is moved from -7.34 to -9.20 eV, and, the character of the latter band is changed from Al $3s$ to H $1s$ character. The Al $3s$ bands are located in a wide energy range from -2.8 to -7.34 eV in Th_2Al and are in a narrow energy range from -2.5 to -4.2 eV in the hydride. The drastic change in the Al bands on hydrogenation of Th_2Al is due to the electron transfer from H to Al and this is discussed further in Sec. III E. The H s bands are found in the energy range from -2 eV to the bottom of the valence band. Their contribution at E_F is negligibly small indicating the formation of localized bands. The bands at E_F is dominated by the Al $3p$ and Th $6d$ electrons in both Th_2Al and Th_2AlH_4 . Owing to the creation of the pseudogap feature near E_F , the contribution of the Al $3p$ electrons to the bands at E_F level are significantly reduced by the hydrogenation of Th_2Al .

E. Nature of Chemical Bonding

1. Density of state

In order to obtain a deeper insight into the changes in chemical bonding behavior on hydrogenation of Th_2Al we give the angular-momentum and site-decomposed DOS for Th_2Al and Th_2AlH_4 in Fig. 6. DOS features for Th_2Al and Th_2AlH_4 show close similarity. Both exhibit metallic character since there is finite DOS at E_F . From the DOS histogram we see that E_F is systematically shifted towards higher energy in Th_2AlH_4 . This is due to the increase in the number of valence electrons when Th_2Al is hydrogenated. DOS for both Th_2Al and Th_2AlH_4 lie mainly in four energy regions (a) the lowest region around -20 eV stems mainly from localized or tightly bound Th $6p$ states, (b) the region from -9.25 to -2.5 eV originates from bonding of H $1s$, Al $3p$ and Th $6d$ (Th- $6d$ and Al- $3p$ states in Th_2Al), (c) the region from -2.5 to 0 eV comes from bonding states of Al $3p$ and Th $6d$ and (d) the energy region just above E_F (0 to 3.5 eV) are dominated by unoccupied Th $4f$ states.

The semi-core Th $6p$ states are well localized and naturally their effect on bonding is very small. On comparing the Th $6p$ DOS of Th_2Al and Th_2AlH_4 , it is seen that the width is significantly reduced in Th_2AlH_4 owing to the lattice expansion and the inclusion of additional energy levels below E_F . In the valence band region, the band width and DOS are larger for Th_2AlH_4 than for Th_2Al . Hydrogenation enhances interaction between neighboring atoms and thereby increases the overlap of orbitals and in turn results in the enlarged valence band width in Th_2AlH_4 . In particular, the strong hybridization between Th $6d$ and H $1s$ states increases the valence band width from 7.1 eV in Th_2Al to 8.4 eV in Th_2AlH_4 . Th $6d$, Al $3p$ and H $1s$ states are energetically degenerate in the valence band region indicating a possibility of covalent Th-H, Th-Al and Al-H bonds. However, the spatial separation Th-Al (3.22 Å) and Al-H (3.02 Å) is larger than Th-H (2.26 Å). Therefore, covalent bonds between the former part is small whereas there is a significant covalent contribution between Th and H. In conformity with this the COHP and charge density analyses show directional bonding between Th and H (see Sec. III E 2 and III E 3). The accommodation of H in the interstitial position between Th and Al creates new bonding states between Th and H. This also enhances Th-Al distance around 2.2% compared with that in Th_2Al . The consequence of this enhancement is that the Al DOS at the valence band region becomes

narrow and the splitting between the Al $3s$ and $3p$ states is almost doubled (see Fig.6). The finite DOS at E_F which gives the metallic character of Th_2Al and Th_2AlH_4 comes from Th d states in addition to some states of Al p character.

Another interesting feature of the total DOS of Th_2AlH_4 is presence of a deep valley around E_F which is termed as a pseudogap. Pseudogap features are formed not only in crystalline solids³⁴ but occur also in amorphous phases³⁵ and quasicrystals.³⁶ Two mechanisms have been proposed for occurrence of pseudo gap in binary alloys, one attributed to ionic features and the other to the effect of hybridization. Although the electronegativity differences between Th, Al and H are noticeable, they are not large enough to explain the pseudogap in Th_2AlH_4 . Hence hybridization must be the cause for creation of the pseudogap in Th_2AlH_4 . There is a correlation between the occurrence of pseudogaps and structural stability³⁷, that materials which possess pseudogaps in the vicinity of E_F usually have higher stability. This may be the reason for the higher value of ΔH in Th_2AlH_4 than in Th_2Al (Table III).

2. Charge density

The analysis of the bonding between the constituents will give better understanding about the anisotropic changes in the structural parameters on hydrogenation of Th_2Al . Fig. 7) shows the calculated valence charge density (obtained directly from the self-consistent calculation) within ab and ac planes for Th_2AlH_4 . Th, Al and H atoms are confined to layers along c , Th and Al being situated in alternating metal layers with hydrogen in between, hence establishing a sequence of Th-H-Al-H-Th-H-Al-H-Th layers (see Fig. 1). The H atoms are arranged in a chain like manner within the ab plane as also evident from Fig. 7b. It is interesting to note that the nature of H-H bonding is quite different along a and c . Although the H-H distance is 2.34 Å within the basal plane and 1.95 Å perpendicular to the basal plane, the bonding between the H atoms is not totally dominated by the latter interactions. In fact the COHP analysis (sec. III E 3) shows that the covalent H-H interaction within the ab plane is larger than within ac plane. The electron distribution between Al and H suggests ionic bonding between them, in line with their electronegativity difference of 0.7. In conformity with this the integrated charge inside the Al sphere is around 0.59 (0.8 according to the TBLMTO method) electrons larger in Th_2AlH_4 than in Th_2Al .

The bonding between Th and H is predominantly covalent as evidenced by the finite charge between these atoms. The H- s electrons are tightly bound to the Th- d states, and Th-H arrangement forms a H-Th-H dumb-bell pattern. Now we will try to obtain a possible explanation for the short H-H distance within ac plane of Th_2AlH_4 from the charge density analysis. The strong covalent interaction between Th and H in the ac plane(see Fig. 7b) and the dumb-belled pattern tend to draw the electrons of H towards Th leaving only a small amount of electrons between the H along c to repel each other. The main reason for this short H-H distance is then reduced repulsion rather than bonding interaction between them.

3. COHP

COHP is an extremely useful tool to analyze covalent bonding interaction between atoms, the simplest approach being to investigate complete COHP between the atoms concerned, taking all valence orbitals into account. COHP between Th-H, Th-Al, Al-H and H-H in Th_2AlH_4 are given in Fig. 9.

Owing to the very different interatomic distances between the H atoms in the *ab* and *ac* planes, special attention is paid to COHP in these planes. Both bonding and antibonding states are present almost equally in the VB region indicating that covalent interaction between the H atoms is not participating significantly to the stability of Th_2AlH_4 . On the other hand, the bonding states are present in the whole VB region in COHP of Th-Al and Th-H indicating that covalent interaction between these pairs is contributing to structural stability. The presence of the large bonding states in the VB region of COHP for Th-H is the main reason for large value of heat of formation for Th_2AlH_4 compared with Th_2Al . In order to quantify the covalent interaction between constituents of Th_2AlH_4 we have integrated the COHP curves up to E_F for Th-Al, Th-H and Al-H giving -0.778 , -1.244 and -0.072 , respectively. Owing to the presence of both bonding and antibonding states below E_F in COHP the integrated value for H-H becomes negligibly small (-0.086 and -0.011 within the *ac* and *ab* plane, respectively, but as the integrated value of bonding states alone is -0.571 and -0.136 respectively, the bonding H-H interaction is quite different in the two planes). Hence, one can conclude that the bond strength between the constituents of Th_2AlH_4 decrease in the order $\text{Th-H} > \text{Th-Al} > \text{Al-H} > \text{H-H}$.

The experimental^{5,9} and theoretical studies show highly anisotropic changes in the lattice expansion on hydrogenation of Th_2Al . According to the crystal structure of Th_2Al the interatomic distance between the interstitial regions where one can accommodate H in the *ab* plane is 2.4 \AA . Hence, there is a large flexible space for accommodation of the H atoms in this plane without the need to expand the lattice. In contrast, the interatomic distance between the interstitial regions in the *ac* plane is only 1.65 \AA . So, large expansion of the lattice along *c* is necessary to accommodate H within the *ac* plane. As a result, even with a short H-H separation of 1.95 \AA , a volume expansion of 12.41% is needed when Th_2AlH_4 is formed from Th_2Al . The experimental observation of 0.105% lattice expansion along *a* and 12.15% along *c* is found to be in excellent agreement with theoretically obtained value of 0.03 and 12.41% , respectively.

IV. CONCLUSION

This study reports a detailed investigation on the electronic structure, bonding nature and ground state properties of Th_2Al and Th_2AlH_4 using first-principle method. The following important conclusions are obtained.

- 1) Th_2Al and Th_2AlH_4 are formed in the CuAl_2 -type crystal structure, the optimized atomic positions and lattice parameters are in very good agreement with recent experimental results.
- 2) Structural optimization gave a shortest H-H separation of 1.95 \AA , which is close to the recent experimental value of 1.97 \AA .

- 3) We observed a highly anisotropic volume expansion of 12.47% of the Th₂Al matrix on hydrogenation to Th₂AlH₄, of which 99.76% volume expansion occurs perpendicular to the basal plane and negligible change along the basal plane.
- 4) The large difference in interatomic distance between the interstitial regions within the *ab* and *ac* planes and the strong covalent interaction between Th and H along *c* keeps the H atoms close together in the *c* direction. This is the main reasons for highly anisotropic volume expansion on hydrogenation in Th₂Al.
- 5) Charge density and COHP analysis revealed that the Th-H bonds are stronger than the H-H bonds and other localized bonds in this structure. The formation of strongly bonded ThH₂ subunits in Th₂AlH₄ makes repulsive interaction between the H atoms smaller along *c* and this is the precise reason for the violation of 2 Årule.
- 6) There is a correlation between *c/a* and the structural stability of hydrated CuAl₂-type phases. For phases with *c/a* < 0.825 the symmetry changes from *I*₄/*mcm* to *P*₄/*ncc* on hydrogenation, whereas for *c/a* > 0.825 the crystal symmetry is not affected on hydrogenation.
- 7) Density of states and bandstructure studies show that Th₂Al and Th₂AlH₄ are having non vanishing N(E_F), resulting in metallic character. The cohesive energy analysis show that, Th₂AlH₄ is more stable than Th₂Al.

ACKNOWLEDGMENTS

P.V. gratefully acknowledges Prof. Karlheinz Schwarz, Prof. Peter Blaha, Prof. O.K. Andersen and Prof. O. Jepsen for supplying computer codes used in this study. The authors also acknowledge Dr. Florent Boucher for useful discussion on COHP. This work has received support from The Research Council of Norway (Programme for Supercomputing) through a grant of computing time.

TABLES

TABLE I. Atomic position of Th₂Al and Th₂AlH₄

	Th ₂ Al			Th ₂ AlH ₄		
	<i>x</i>	<i>y</i>	<i>z</i>	<i>x</i>	<i>y</i>	<i>z</i>
Th Theory	0.1583	0.6583	0.0000	0.1632	0.6632	0.0000
Exp. ¹⁷	0.1588	0.6588	0.0000	–	–	–
Exp. ⁹	–	–	–	0.1656	0.6656	0.0000
Exp. ⁵	–	–	–	0.162	0.662	0.0000
Al Theory	0.0	0.0	0.25	0.0	0.0	0.25
Exp. ¹⁷	0.0	0.0	0.25	–	–	–
Exp. ⁹	–	–	–	0.0	0.0	0.25
Exp. ⁵	–	–	–	0.0	0.0	0.25
H Theory	–	–	–	0.3705	0.8705	0.1512
Exp. ⁹	–	–	–	0.3707	0.8707	0.1512
Exp. ⁵	–	–	–	0.368	0.868	0.137

TABLE II. Lattice parameters and inter atomic distances of Th₂Al and Th₂AlH₄(all values are in Å).

	Th ₂ Al		Th ₂ AlH ₄		
	Theory	Exp. ¹⁷	Theory	Exp. ⁹	Exp. ⁵
<i>a</i>	7.602	7.618	7.604	7.626	7.629
<i>c</i>	c = 5.723	5.862	6.433	6.515	6.517
<i>c/a</i>	0.753	0.769	0.846	0.854	0.854
Th-H	–	–	2.273	2.305	2.387
Th-Al	3.199	3.219	3.269	3.278	3.291
Th-Th	3.403	3.421	3.509	3.571	3.495
Al-H	–	–	3.051	3.061	3.072
Al-Al	2.861	2.931	3.216	3.257	3.258
H-H (<i>ac</i> -plane)	–	–	1.945	1.971	1.790
H-H (<i>ab</i> -plane)	–	–	2.344	2.305	2.495

TABLE III. Ground state properties of Th₂Al and Th₂AlH₄

Compound	Th ₂ Al	Th ₂ AlH ₄
– ΔH (in kJ mol ^{–1})	18.35	29.50
E_{coh} (eV/atom)	0.15	0.185
$N(E_F)$ (states/Ry-cell)	58.42	41.13
B_0 (GPa)	93.42	111.36
B'_0	3.41	3.48

FIGURES

FIG. 1. The crystal structure of Th_2AlH_4 . Five Th in face sharing tetrahedral configuration surrounding two hydrogen. Legends to the different kinds of atoms are given on the illustration.

FIG. 2. Total energy (a) *vs.* c/a and (b) *vs.* unit cell volume for Th_2Al where $\Delta E = E + 106632$.

FIG. 3. The total energy (a) *vs.* c/a and (b) *vs.* unit cell volume for Th_2AlH_4 where $\Delta E = E + 106636$.

FIG. 4. c/a for CuAl_2 -type phases and their corresponding hydrides.

FIG. 5. Electronic band structure of (a) Th_2Al and (b) Th_2AlH_4 . The Fermi level is set to zero.

FIG. 6. Total, site and orbital projected density of states for (a) Th_2Al and (b) Th_2AlH_4 .

FIG. 7. Valence electron charge density plot for Th_2AlH_4 in the ab plane with 40 contours drawn between 0 and 0.25 electrons/a.u.³

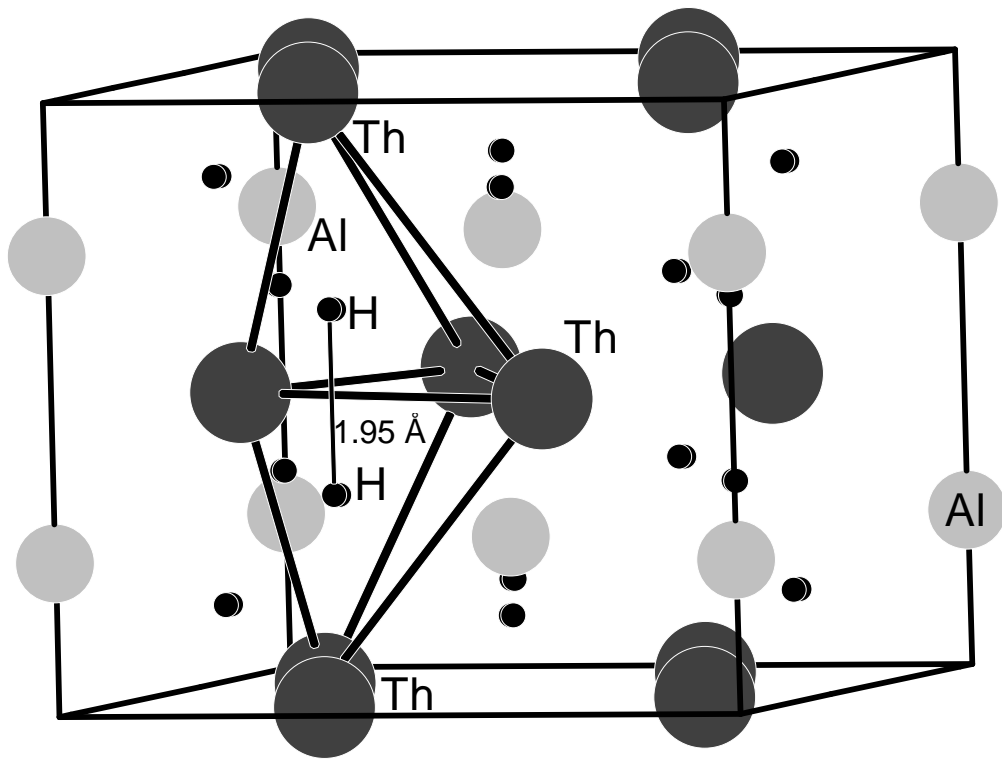
FIG. 8. Valence electron charge density plot between the Th and H atoms for Th_2AlH_4 in the ac plane with 40 contours drawn between 0 and 0.25 electrons/a.u.³.

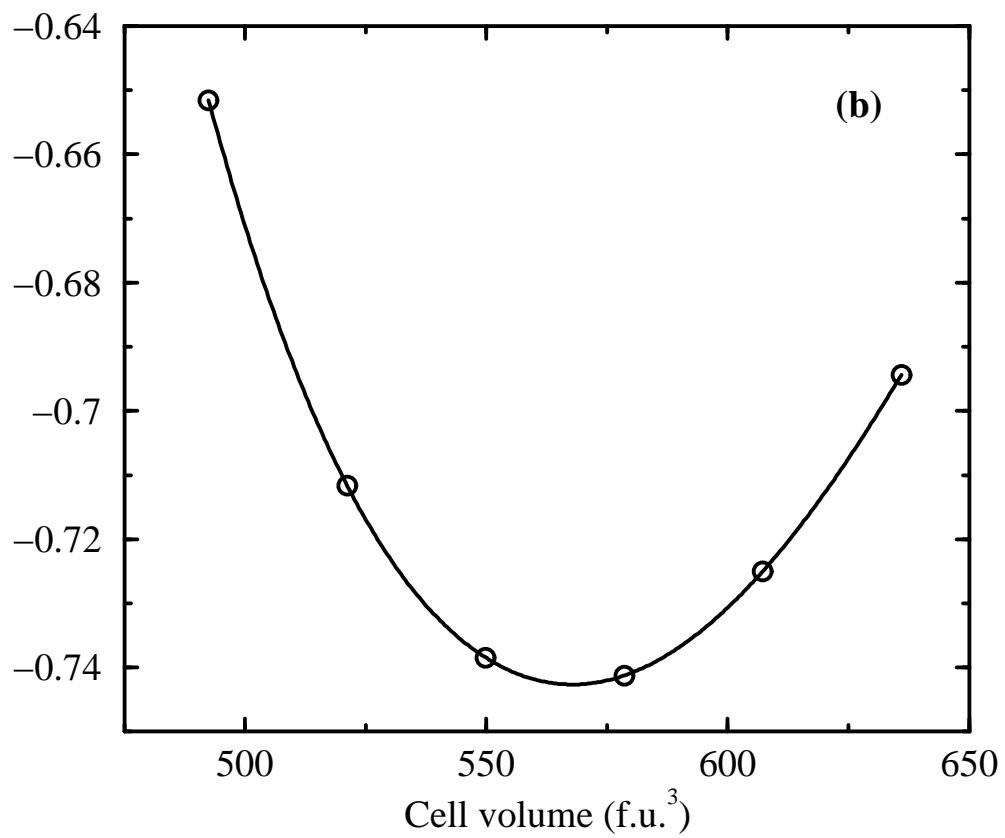
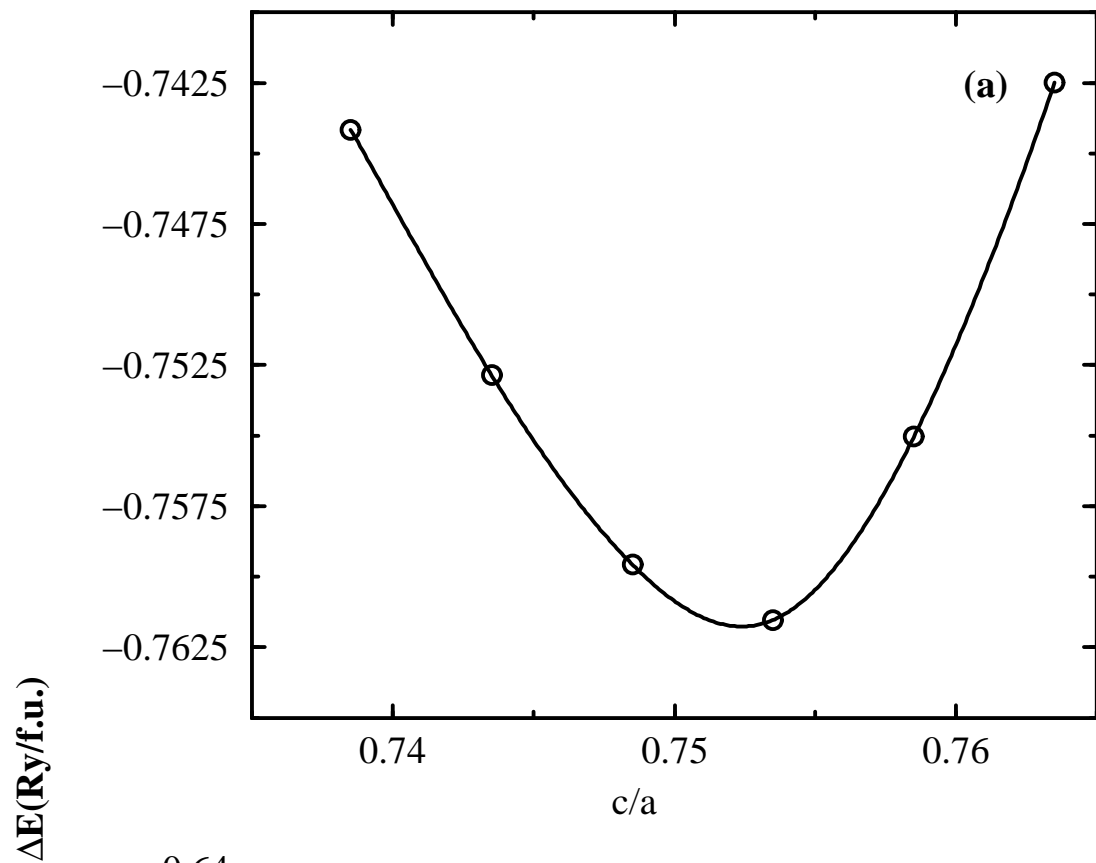
FIG. 9. COHP of Th_2AlH_4 , depicting the contributions from Th-Al, Th-H, Al-H and H-H interactions. The COHP for H atoms in the ab plane and ac plane are given in solid line and dotted lines respectively.

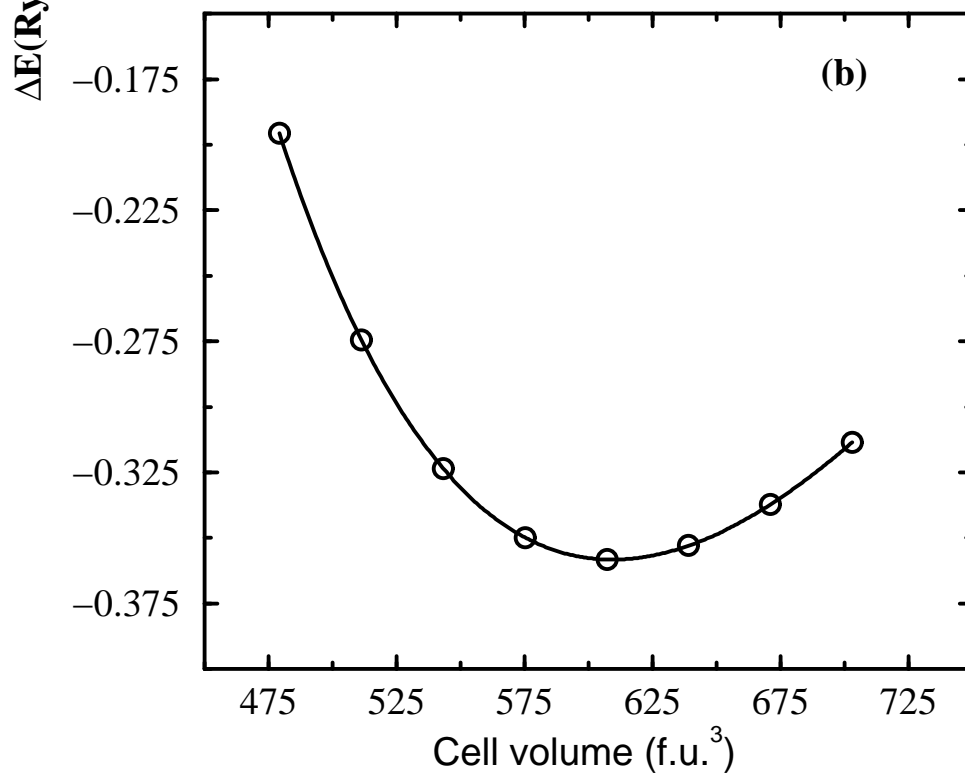
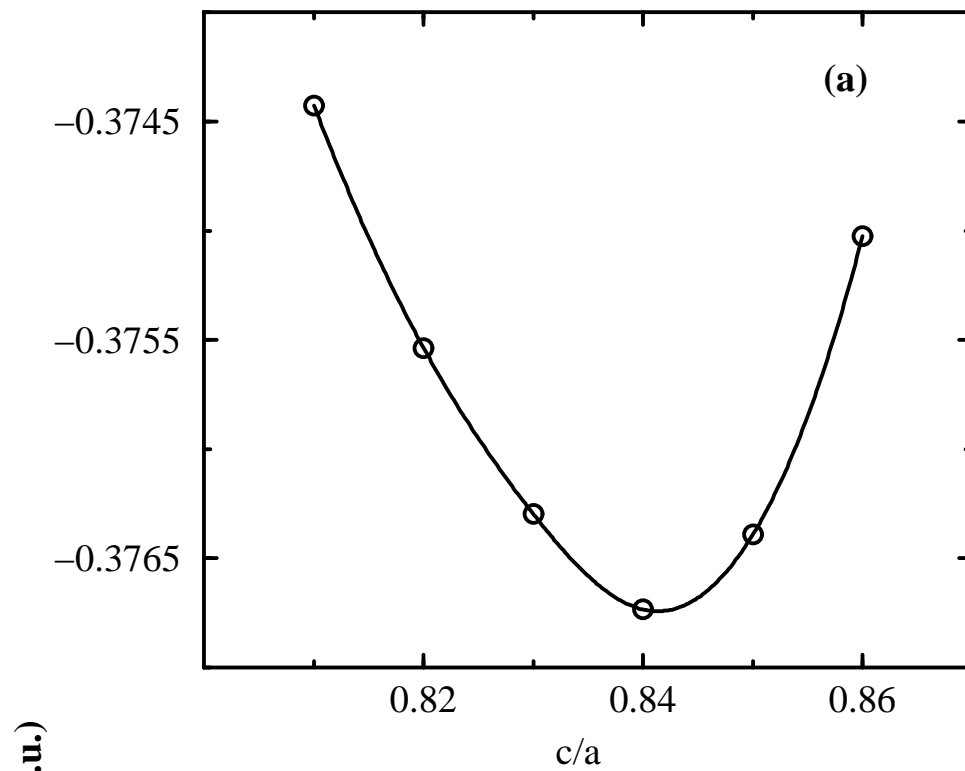
REFERENCES

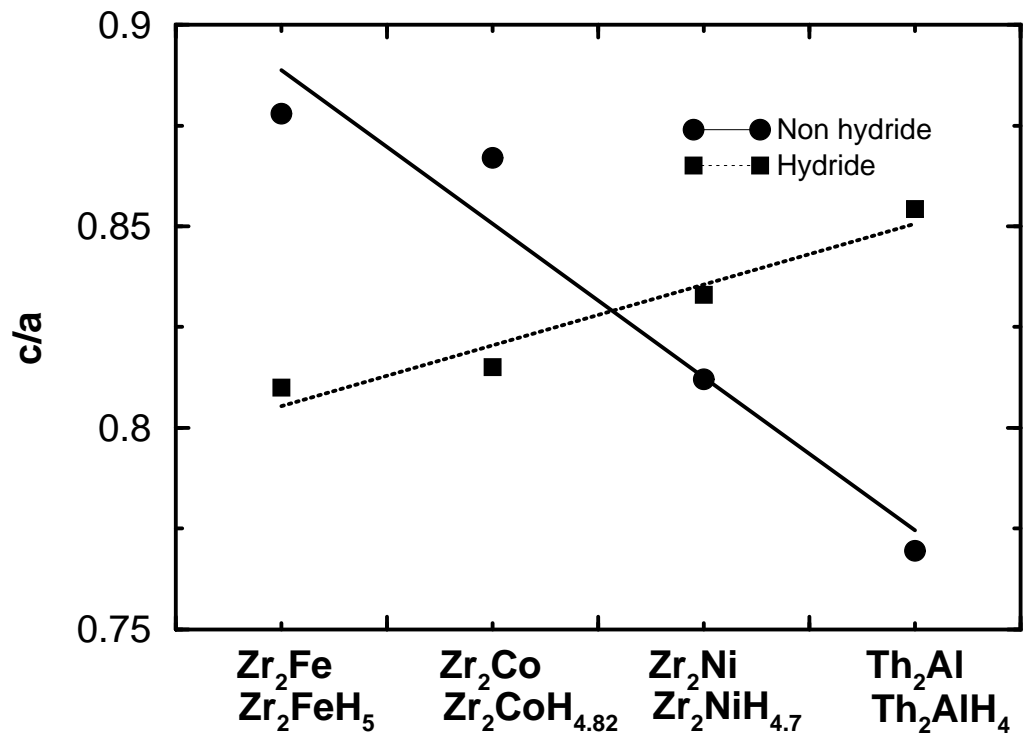
- * electronic address: ponniah.vajeeston@kjemi.uio.no
- ¹ B.K. Rao and P. Jena, Phys. Rev. B **31**, 6726 (1985).
 - ² D. G. Westlake, J. Less Common Met. **103**, 203 (1984).
 - ³ C. Switendick, Z. Phys. Chem. NF B **117**, 89 (1979).
 - ⁴ K. Yvon and P. Fischer, in *Hydrogen in Intermetallic Compounds*, Topics in Applied Physics, Edited by L.Schlapbach **63**, Springer, Berlin 1988, p.87.
 - ⁵ J. Bergsma, J. A. Goedkoop, and J. H. N. van Vucht, Acta Crystallogr. **14**, 223 (1961).
 - ⁶ S. C. Abrahams, A. P. Ginsberg, and K. Knox, Inorg. Chem. **3**, 558 (1964). K. Knox and A. P. Ginsberg, *ibid.* **3**, 555 (1964).
 - ⁷ E. E. Havinga, H. Damsama and P. Hokkeling, J. Less Common Met. **27**, 169 (1972).
 - ⁸ V. A. Yartys, H. Fjellvåg, B. C. Hauback, and A. B. Riabov, J. Alloys and compounds. **274**, 217 (1998).
 - ⁹ M. H. Sørby, H. Fjellvåg, B. C. Hauback, A. J. Maeland, and V. A. Yartys, J. Alloys Comp. **309**, 154 (2000).
 - ¹⁰ A. Chikdene, A. Baudry, P. Boyer, S. Miraglia, D. Fruchart, and J. L. Soubeyroux, Z. Phys. Chem. NF **163**, 219 (1989).
 - ¹¹ H. Nakamura, D. Nguyen-Manh, and D. G. Pettifor, J. Alloys Comp. **281**, 81 (1998).
 - ¹² J. J. Murray, M. L. Post, and J. B. Taylor, J. Less Comm. Met. **80**, 211 (1981).
 - ¹³ B. S. Bowerman, C. A. Wulf, and T. B. Flanagan, Z. Phys. Chem. **116**, 197 (1979).
 - ¹⁴ W. N. Hubbard, P. L. Rawlins, P. A. Connick, R. E. Stedwell, and P. A. G. O. Hare, J. Chem. Thermo. **13**, 785 (1983).
 - ¹⁵ F. Boucher and R. Rousseau, Inorg. Chem. **37**, 2351 (1998).
 - ¹⁶ R. Dronskowski and P. E. Blochl, J. Phys. Chem. **97**, 8617 (1993).
 - ¹⁷ P. Villars and L. D. Calvert, *Pearson's Handbook of Crystallographic Data for Intermetallic Phases*. 2nd ed. Vol.3. ASM International, Materials Park, Ohio.
 - ¹⁸ P. Blaha, K. Schwarz, and J. Luitz, WIEN97, Vienna Univ. of Tech.1997. (An improved and updated Unix version of the original copyrighted by P. Blaha, K. Schwarz and S. B. Trickey), Comput. Phys. Commun., **59**, 399 (1990).
 - ¹⁹ D. Singh, *Plane Waves, Pseudopotentials, and the LAPW Method*, (Kluwer Academic, New York 1994).
 - ²⁰ J.P. Perdew in *Electronic Structure of Solids*, edited by P. Ziische and H. Eschrig (Akademie Verlag, Berlin, 1991), p.11; J.P. Perdew, K. Burke and Y. Wang, Phys. Rev. B **54**, 16533 (1996); J.P. Perdew, K. Burke and M. Ernzerhof, Phys. Rev. Lett. **77**, 3865 (1996).
 - ²¹ D. Singh, Phys. Rev. B, **43**, 6388 (1991).
 - ²² P.E. Blochl, O. Jepsen, and O. K. Andersen, Phys. Rev. B **49**, 16223 (1994).
 - ²³ O. K. Andersen, Phys. Rev. B **12**, 3060 (1975). O. K. Andersen, and O. Jepsen, Phys. Rev. Lett. B **53**, 2571 (1984). H. L. Skriver, *The LMTO method* (Springer, Heidelberg 1984).
 - ²⁴ G. Krier, O. Jepsen, A. Burkhardt, and O. K. Andersen, *Tight binding LMTO-ASA Program Version 4.7*, Stuttgart, Germany (2000).
 - ²⁵ P. Ravindran, G. Subramoniam, and R. Asokamani, Phys. Rev. B **53**, 1129 (1996).
 - ²⁶ C. Ravi, P. Vajeeston, S. Mathijaya, and R. Asokamani, Phys. Rev. B **60**, 15 683 (1999).
 - ²⁷ P. Vajeeston, P. Ravindran, C. Ravi, and R. Asokamani, Phys. Rev. B **63**, 045115 (2001).

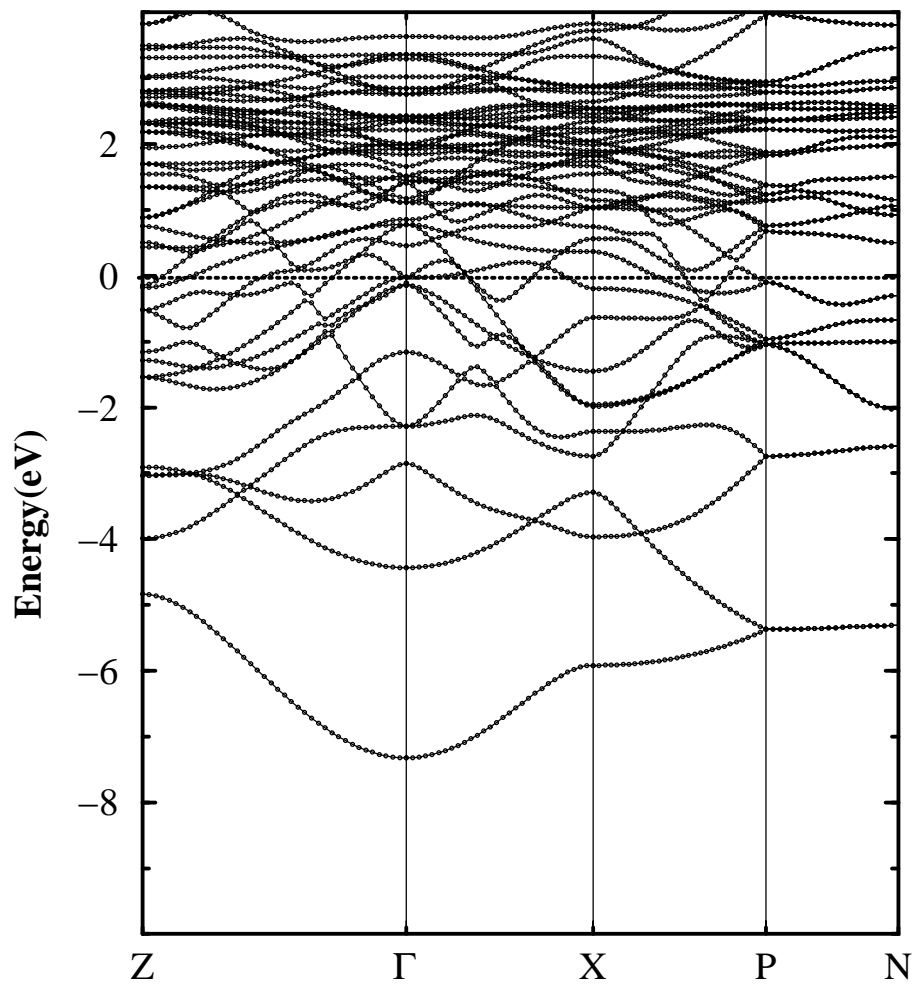
- ²⁸ O. Gunnarsson, *Int. J. Quantum Chem.* **10**, 307 (1976).
- ²⁹ H. H. Van Mal, K. H. Buschow, and A. R. Miedema, *J. Less Comm. Met.* **35**, 65 (1973).
- ³⁰ J. Osterwalder, T. Riesterer, L. Schlapbach, F. Vaillant, and D. Fruchart, *Phys. Rev. B* **31**, 8311 (1985).
- ³¹ L. Schlapbach, F. Meli, and A. Zuttel in *Intermetallic compounds*, edited by J. H. Westbrook and R. L. Fleischer (Wiley, New York, 1994), Vol. 2, Chap. 21, pp. 475-488.
- ³² F. Bonhomme, K. Yvon, and M. Zolliker, *J. Alloys Comp.* **199**, 129 (1993).
- ³³ M. M. Elcombe, S. J. Campbell, C. J. Howard, H. G. Buttner, and F. Aubertin, *J. Alloys Comp.* **232** 174 (1999).
- ³⁴ J. H. Xu and A. J. Freeman, *Phys. Rev. B* **41**, 12553 (1990).
- ³⁵ A. Pasturel, C. Colinet, and P. Hicter, *Physica B* **132**, 177 (1985).
- ³⁶ J. C. Phillips, *Phys. Rev. B* **47**, 2522 (1992).
- ³⁷ P. Ravindran and R. Asokamani, *Bulletin-of-Materials-Science*, **20**, 613 (1997); V. L. Moruzzi, P. Oelhafen and A. R. Williams, *Phys. Rev. B* **27**, 7194 (1983).



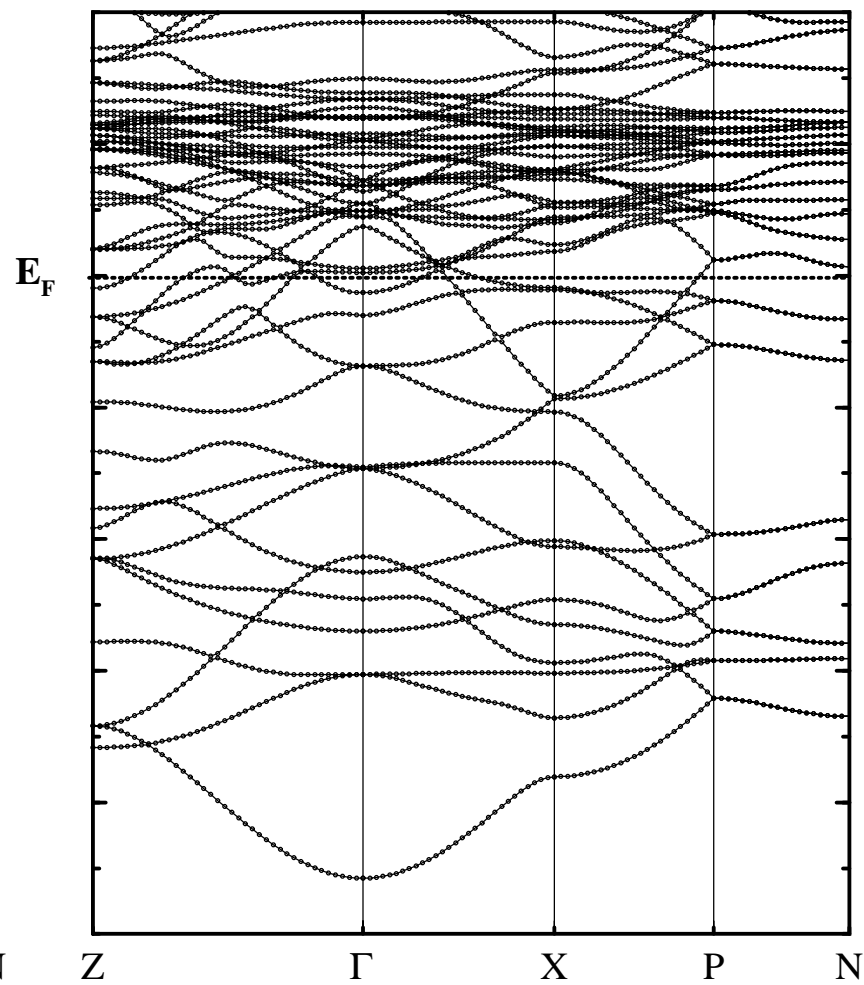




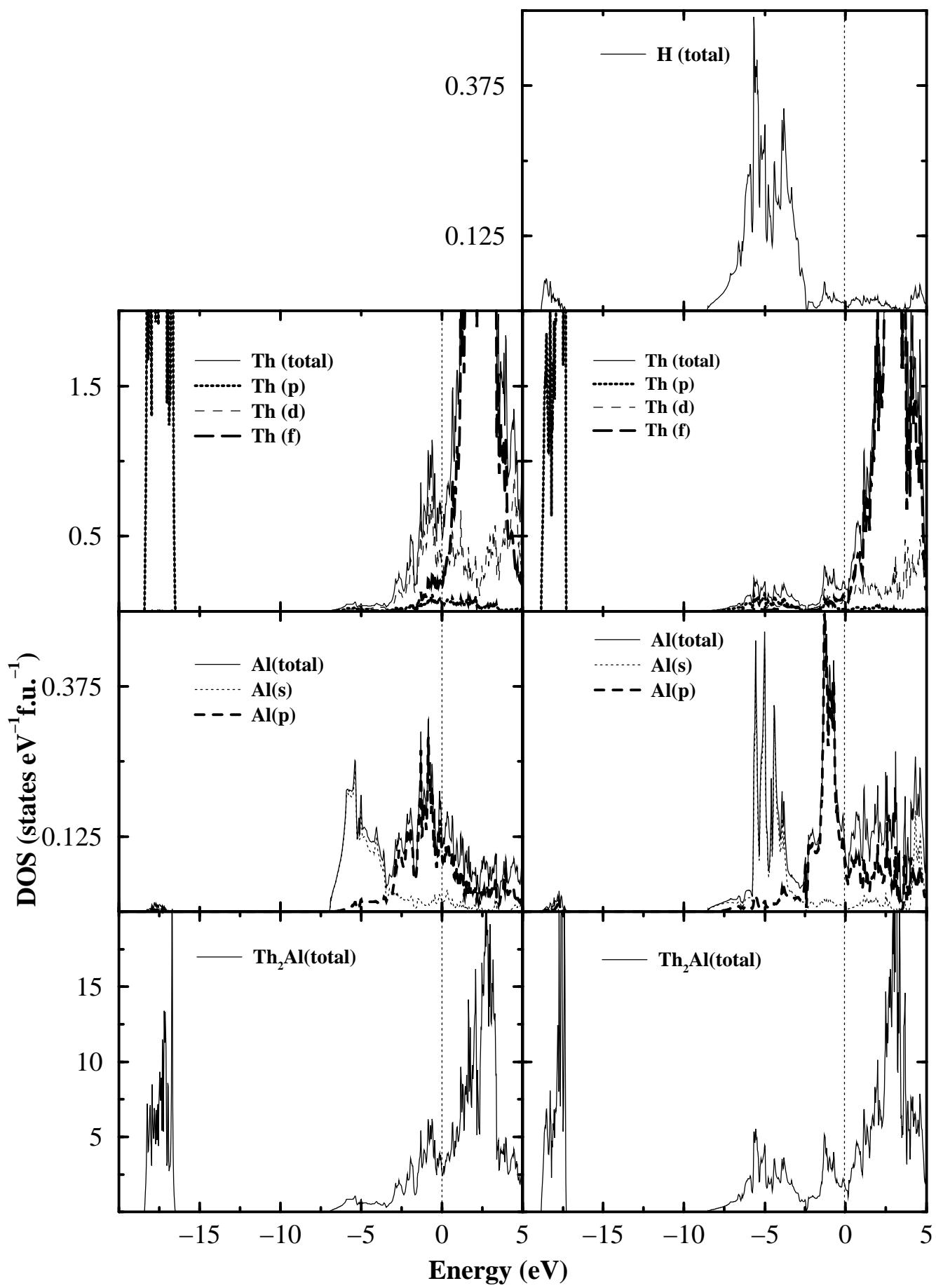




(a)



(b)



This figure "fig7.jpg" is available in "jpg" format from:

<http://arxiv.org/ps/cond-mat/0108278v1>

This figure "fig8.jpg" is available in "jpg" format from:

<http://arxiv.org/ps/cond-mat/0108278v1>

